Pharmaceutical Research, Vol. 5, No. 9, 1988

Research Article

Kinetics of Release from Enteric-Coated Tablets

Sadettin S. Ozturk,[1] Bernhard O. Palsson,[1] Bruce Donohoe,[2] and Jennifer B. Dressman[3,4]

Received September 21, 1987; accepted March 9, 1988

Controlled and localized release of drugs in the intestine can be achieved by enteric coating. The design of enteric-coated tablets has so far remained empirical, in part because of the lack of a quantitative description of the drug release kinetics. In this paper, a mathematical model is presented that describes the dissolution of the polymer coating and release kinetics of weakly acidic drugs from enteric-coated tablets in buffered media. This model can also be used to predict the time of onset of core disintegration. The model assumes that the release rate is limited by diffusion, and furthermore, all the reactions are considered as reversible and instantaneous. Dissolution and reaction are assumed to take place in the polymer layer and a hypothetical stagnant liquid film adjacent to the polymer layer (the classical film theory approach). The dissolution of the enteric coating is found to depend on the intrinsic solubilities and pK_a's of the drug and polymer and the medium properties. The release rate of the drug is found to depend on the intrinsic solubilities and pK_a's of drug and polymer, the medium properties, i.e., pH and buffer capacity, and a mass transfer coefficient. Explicit relationships between the release rates and all these factors are derived. Successful prediction of experimental data indicates that the model provides an adequate description of release from enteric coated tablets. Limitations of the model and its potential application to the design of appropriate *in vitro* testing conditions and to the formulation of enteric coated tablets are also discussed.

KEY WORDS: Enteric coating; release kinetics; film model; disintegration time; formulation design.

INTRODUCTION

Enteric coating of drug tablets is used to prevent the release of drugs in the stomach, either to reduce the risk of gastrointestinal side effects or to maintain the stability of drugs which are subject to degradation in the gastric environment (1). An important example is enteric coating of aspirin to protect the gastric mucosa from corrosion. This application is particularly important for those on chronic aspirin medication, e.g., for arthritic patients. Erythromycin, pancreatin, potassium chloride, and diethylstilbestrol are other examples of drugs that have been formulated as enteric-coated products (2).

An enteric-coated dosage form should not allow significant release of drug in the stomach yet provide rapid dissolution of the polymer layer and complete release of drug at the desired site in the intestine. Most polymers used for enteric coating are polyacids, whose solubilities in aqueous media are strongly pH dependent.

Cellulose acetate phthalate (CAP), polyvinylacetate phthalate (PVAP), and methacrylic acid/methylmethacrylate copolymers are often used for enteric coating. These polymers are weak acids, containing carboxyl groups in a substantial proportion of their monomeric units (Fig. 1). Rapid dissolution of these polymers thus requires pH values that are much higher than normally present in the stomach. However, when hydrated these polymers are permeable to the confined drug even at pH's lower than the dissolution pH. Important factors in the design of enteric-coated dosage forms include the choice of an appropriate polymer and the specification of the thickness of the polymer layer.

The standard basis for determining the efficacy of an enteric-coated tablet is the 1985 USP modified disintegration test (4). This test requires that the product remain physically intact for a specified period when exposed to simulated gastric fluid (SGF) and yet disintegrate readily in simulated intestinal fluid (SIF). Recently the test for enteric-coated aspirin tablets was changed to a dissolution test (4). A poor correlation between the 1985 USP tests and *in vivo* performance has been demonstrated (5). A more quantitative understanding of the release mechanism should provide a basis for developing a more predictive *in vitro* test.

Drug release has been modeled for a variety of dosage forms and conditions for the purposes of determining the factors that affect the drug release and predicting the temporal profile of drug release. Nernst (6) modeled the dissolution of drug from the pure solid using the classical film theory for mass transfer. The resulting dissolution rate, J, of a nonionized drug, is expressed as a product of a "driving force" and a "resistance":

$$J = \frac{D}{\delta}(C_0 - C_b) = k_s \Delta C \qquad (1)$$

[1] Department of Chemical Engineering, The University of Michigan, Ann Arbor, Michigan 48109.
[2] Department of Anatomy and Cell Biology, The University of Michigan, Ann Arbor, Michigan 48109.
[3] College of Pharmacy, The University of Michigan, Ann Arbor, Michigan 48109-1065.
[4] To whom correspondence should be addressed.

0724-8741/88/0900-0550$06.00/0

Cellulose Acetate Phthalate (CAP)

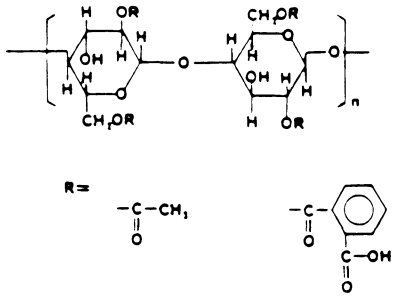

PolyVinyl Acetate Phthalate (PVAP)

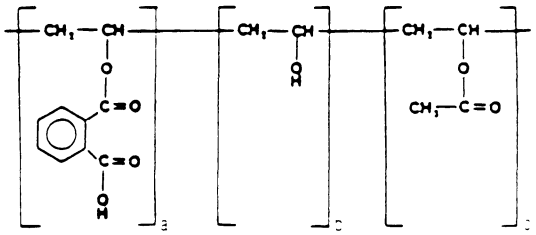

Methacrylic acid/methylmethacrylate co-polymer

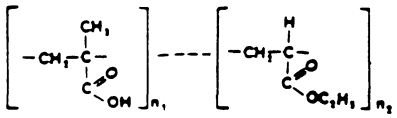

Fig. 1. Chemical structure of some polymers used for enteric coating (reproduced with permission from Ref. 3).

where C_0 and C_b are the concentrations of drug at the surface (intrinsic solubility) and in the bulk fluid, respectively, D is the diffusivity of the dissolving species, and δ is the diffusion layer thickness. Furthermore $k_s(=D/\delta)$ is defined as the mass transfer coefficient, and $\Delta C = (C_0 - C_b)$ is the driving force. If the hydrodynamics are known, all values in Eq. (1) can be obtained *a priori,* thus permitting prediction of dissolution rates.

For ionizable drugs the analysis becomes more complex because of the reactions that occur. Mathematical modeling of such systems was initiated by Brunner (7) and extended later by Higuchi *et al.* (8,9) and Mooney *et al.* (10,11). Recently Ozturk *et al.* (12) developed simple and explicit expressions for dissolution of both weak acids and weak bases in buffered and unbuffered aqueous solutions. Dissolution rates were found to be of the same mathematical form as Eq. (1), except that the intrinsic solubilities (C_0) had to be replaced by the total solubilities ($C_{T,s}$), defined as follows:

For weak acids,

$$C_{T,s} = C_0\left(1 + \frac{K_a}{[H^+]_s}\right) \tag{2}$$

For weak bases,

$$C_{T,s} = C_0\left(1 + \frac{[H^+]_s}{K_a}\right) \tag{3}$$

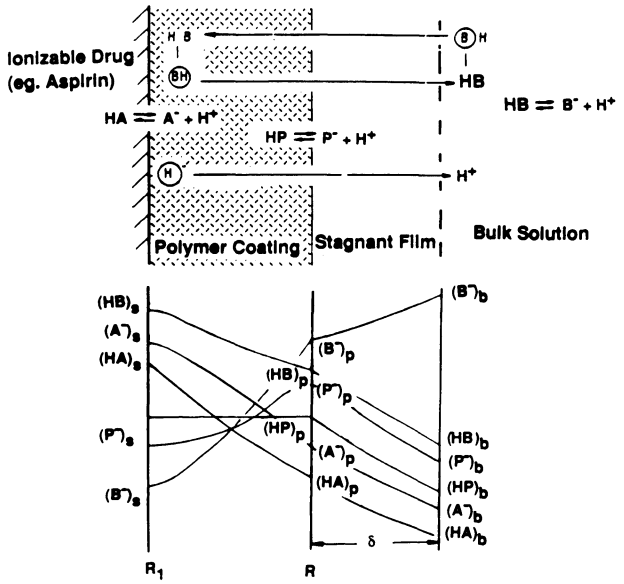

Fig. 2. Schematic representation of polymer dissolution and drug release from enteric-coated tablets.

where $[H^+]_s$ is the hydrogen ion concentration at the solid surface.

Dissolution of polymer from free films has been modeled (e.g., Ref. 13) by a method analogous to that of Higuchi *et al.* (8,9). For enteric-coated dosage forms, however, dissolution of the polymer layer may be modified by interaction with the drug and excipients. Although experimental results for drug release from enteric coated dosage forms have appeared in the literature (e.g., Refs. 14 and 15), a corresponding mathematical analysis has yet to appear.

The objective of this work is to model the release kinetics from enteric-coated dosage forms in buffered media. The important parameters affecting the release rate of drug, dissolution of the polymer, and onset of tablet disintegration are identified. The model is used to predict the release rate of drug under various medium conditions and the results are compared with experimental data. The analysis is subsequently applied to the design of enteric-coated tablets.

THEORETICAL

Figure 2 is a diagram of the concentration profiles during the dissolution of a weak acid HA confined by an enteric coating polymer HP. HB is used to designate the buffer; A^-, P^-, and B^- represent the ionized form of the drug, the polymer, and the base conjugate of the buffer, respectively. B^- indicates that the base conjugate of the buffer carries one more negative charge than HB. The polymer has an initial thickness of $h = R_2 - R_1$, surrounding a drug core of radius R_1, and δ is the thickness of the stagnant diffusion layer adjacent to the polymer coating. The two interfaces,[5] at $r = R_1$ and $r = R$, correspond to the drug/polymer and polymer/stagnant diffusion layer interfaces, respectively.

[5] The polymer/diffusion layer interface moves with time from the initial position at R_2, the initial radius of the coated tablet. The position at time t is represented by R.

Subscripts s, p, and b are used to designate the concentrations at the drug surface, the polymer/stagnant diffusion layer interface, and the bulk, respectively. The drug diffuses first through the polymer, then through the stagnant diffusion layer. During this transfer the drug simultaneously reacts with the incoming buffer B^- to yield the conjugate base A^- and HB. The polymer also diffuses away from the polymer–diffusion layer interface and can simultaneously react with basic species. The bulk is assumed to be well mixed and chemical equilibrium attained instantly throughout. The concentration of nonionized polymer [HP] in the polymer region $R_1 < r < R$ is assumed to be constant and equal to its intrinsic solubility, $[HP]_0$. At the drug surface the concentration of nonionized drug [HA] is equal to its solubility, $(HA)_0$, the intrinsic solubility.

The polymer/stagnant diffusion layer interface moves toward the drug core as the polymer dissolves. The thickness of the stagnant film (δ), on the other hand, is governed by the mixing in the bulk and is assumed to be constant (24). Use of the quasi-steady-state approximation simplifies analysis of the moving boundary problem considerably (12). A macroscopic mass balance on the tablet yields

$$-\rho_M \frac{dR}{dt} = J_{HP} \tag{4}$$

where J_{HP} denotes the dissolution flux and ρ_M is the molal density of the polymer. This equation can be used to describe the variation of the polymer thickness with time and hence to calculate the time for onset of disintegration. We now proceed to evaluate J_{HP} based on the film model described above.

General Mass Balances

A complete description of mass transfer for a mixture of reacting species (drug, polymer, and buffer) requires consideration of diffusion, convection, and reaction. If Fick's law of diffusion applies, then the general mass balance for a given species is

$$\frac{\partial C_i}{\partial t} + \mathbf{v} \cdot \nabla C_i = D_i \nabla^2 C_i + \sum_k \nu_{i,k} \phi_k \tag{5}$$

where C_i is the molar concentration, D_i is the diffusion coefficient, v is the fluid velocity vector, t is time, ∇C_i is the concentration gradient, $\nabla^2 C_i$ is the Laplacian operator, ϕ_k is the kth reaction rate and $\nu_{i,k}$ is the stoichiometric coefficient of component i in the kth reaction.

For the description of polymer dissolution and drug release we can neglect some of the terms in this general balance equation.[6]

(i) If the bulk solution is a homogeneous mixture with no significant concentration gradients and all the dissolution processes are confined to a stagnant layer (polymer and diffusion films around the solid drug core) with no convection, the term $\mathbf{v} \cdot \nabla C_i$ disappears.

(ii) If the diffusional response times are rapid relative to the dissolution process, we can use a quasi-steady-state assumption.

(iii) The term $\nabla^2 C_i$ is written in different forms depending on the geometry. The shape of the enteric-coated tablet can be approximated as a sphere with concentration changes in the radial direction.[7]

In these circumstances, we obtain

$$\frac{D_i}{r^2}\frac{d}{dr}\left(r^2 \frac{dC_i}{dr}\right) + \sum_k \nu_{i,k}\phi_k = 0 \tag{6}$$

Next we identify the number of independent chemical reactions. This can be done systematically by a linear algebraic method (e.g., Ref. 25). The reactions are represented in the following matrix notation:

$$\begin{pmatrix} 0 & 0 & 0 & -1 & -1 & 1 & 0 & 0 \\ -1 & 1 & 0 & 0 & 1 & 0 & 0 & 0 \\ -1 & 1 & 0 & 0 & 0 & -1 & 1 & 0 & 0 \\ -1 & 1 & -1 & 1 & 0 & 0 & 0 & 0 \\ 0 & 0 & 1 & -1 & 0 & -1 & 1 & 0 & 0 \\ 0 & 0 & 0 & 0 & 0 & -1 & 1 & -1 & 1 \\ 0 & 0 & -1 & 1 & 0 & 0 & 0 & -1 & 1 \\ 0 & 0 & 0 & 0 & 1 & 0 & 0 & -1 & 1 \end{pmatrix} \begin{pmatrix} HA \\ A^- \\ B^- \\ BH \\ H^+ \\ OH^- \\ H_2O \\ HP \\ P^- \end{pmatrix} = AC = 0 \tag{7}$$

Where A is a matrix of stoichiometric coefficients and C is the concentration vector. Since the matrix A has a rank of four, we have only four independent reactions. We use

$$\begin{aligned} \phi_1&: HA \rightleftharpoons A^- + H^+, & K_a &= [A^-][H^+]/[HA] \\ \phi_2&: HB \rightleftharpoons B^- + H^+, & K_b &= [B^-][H^+]/[HB] \\ \phi_3&: HP \rightleftharpoons P^- + H^+, & K_p &= [P^-][H^+]/[HP] \\ \phi_4&: H_2O \rightleftharpoons OH^- + H^+, & K_w &= [OH^-][H^+] \end{aligned}$$

as our independent reactions, where ϕ_i represents the rate of a given reaction and the K_i's are equilibrium constants.

The mass balance equations for the diffusion layer are

$$\frac{D_{HA}}{r^2}\frac{d}{dr}\left(r^2\frac{d[HA]}{dr}\right) = \phi_1 \tag{8}$$

$$\frac{D_{A^-}}{r^2}\frac{d}{dr}\left(r^2\frac{d[A^-]}{dr}\right) = -\phi_1 \tag{9}$$

$$\frac{D_{B^-}}{r^2}\frac{d}{dr}\left(r^2\frac{d[B^-]}{dr}\right) = -\phi_2 \tag{10}$$

$$\frac{D_{HB}}{r_2}\frac{d}{dr}\left(r^2\frac{d[HB]}{dr}\right) = \phi_2 \tag{11}$$

$$\frac{D_{HP}}{r^2}\frac{d}{dr}\left(r^2\frac{d[HP]}{dr}\right) = \phi_3 \tag{12}$$

$$\frac{D_{P^-}}{r^2}\frac{d}{dr}\left(r^2\frac{d[P^-]}{dr}\right) = -\phi_3 \tag{13}$$

$$\frac{D_{H^+}}{r^2}\frac{d}{dr}\left(r^2\frac{d[H^+]}{dr}\right) = -\phi_1 - \phi_2 - \phi_3 - \phi_4 \tag{14}$$

$$\frac{D_{OH^-}}{r^2}\frac{d}{dr}\left(r^2\frac{d[OH^-]}{dr}\right) = \phi_4 \tag{15}$$

[6] A discussion of the basis for the simplifying assumptions is given elsewhere (12).

[7] Other idealizations are that the coating is of a uniform thickness around the tablet core and that the core is assumed to consist of a solid pure compacted drug.

[8] Note that there is no equation for [HP] in the polymer layer as it assumes a constant value of $[HP]_0$: the intrinsic solubility.

and the analogous equations for the polymer layer are[8]

$$\frac{D'_{HA}}{r^2}\frac{d}{dr}\left(r^2\frac{d[HA]'}{dr}\right) = \phi'_1 \quad (16)$$

$$\frac{D'_{A^-}}{r^2}\frac{d}{dr}\left(r^2\frac{d[A^-]'}{dr}\right) = -\phi'_1 \quad (17)$$

$$\frac{D'_{B^-}}{r^2}\frac{d}{dr}\left(r^2\frac{d[B^-]'}{dr}\right) = -\phi'_2 \quad (18)$$

$$\frac{D'_{HB}}{r^2}\frac{d}{dr}\left(r^2\frac{d[HB]'}{dr}\right) = \phi'_2 \quad (19)$$

$$\frac{D'_{P^-}}{r^2}\frac{d}{dr}\left(r^2\frac{d[P^-]'}{dr}\right) = -\phi'_3 \quad (20)$$

$$\frac{D'_{H^+}}{r^2}\frac{d}{dr}\left(r^2\frac{d[H^+]'}{dr}\right) = -\phi'_1 - \phi'_2 - \phi'_3 - \phi'_4 \quad (21)$$

$$\frac{D'_{OH^-}}{r^2}\frac{d}{dr}\left(r^2\frac{d[OH^-]'}{dr}\right) = -\phi'_4 \quad (22)$$

where $[X]$, $[X]'$ and D_i, D'_i are the concentration and diffusivities in the stagnant diffusion layer and in the polymer matrix, respectively (X represents HA, A^-, B^-, HB, P^-, HP, OH^-, or H^+).

Boundary Conditions

Boundary conditions are needed at three locations.

1. At the drug surface, $r = R_1$, $[HA]' = [HA]_s = [HA]_0$, the intrinsic solubility of the drug, which is a measurable quantity. Provided that the core remains composed predominantly of solid during the polymer dissolution phase, we can then make the assumption that there is no flux of the species other than HA at the core surface, i.e., that there is no penetration of the species into the undissolved solid phase. Hence we use the "no-flux" boundary conditions at the core surface:

$$J_i = D_i\frac{dX}{dr} = 0, \qquad X \neq HA \quad (23)$$

The flux of HA is

$$-D_{HA}\left(\frac{d[HA]}{dr}\right)_{r=R_1} = J_{HA} \quad (24)$$

2. At the polymer/diffusion layer interface, $r = R$, we use the continuity requirement that

$$[X] = [X]' = [X]_p \quad (25)$$

and

$$D_i\frac{d[X]}{dr} = D'_i\frac{d[X]'}{dr} \quad (26)$$

For the dissolving polymer we have the flux condition:

$$-D_{HP}\frac{d[HP]}{dr} = J_{HP} \quad (27)$$

3. At the outer edge of the diffusion layer, $r = R + \delta$, we use the bulk values, i.e.,

$$[X] = [X]_b, \qquad \text{for all } X \quad (28)$$

In most cases of interest the bulk concentration of dissolving drug $[HA]_b$ and $[A^-]_b$ and polymer $[HP]_b$ and $[P^-]_b$ are insignificant and assumed to be negligible, so-called sink conditions.

We further assume that in the region of $R_1 < r < R$ the polymer is free to dissolve and that the concentration of the nonionized form is constant and equal to its intrinsic solubility:

$$[HP]' = [HP]_s = [HP]_p = [HP]_0$$

Solution of Differential Equations

In the mass balance equations the reaction rates, ϕ_i, are not known; hence we cannot integrate them directly to solve for the concentration of individual species. However, the reaction rates can be eliminated by appropriate combination of the mass balance equations.

By adding Eqs. (12) and (13) we get

$$\frac{1}{r^2}\frac{d}{dr}\left[r^2\frac{d}{dr}(D_{HP}[HP] + D_{P^-}[P^-])\right] = 0 \quad (29)$$

eliminating ϕ_3. Integrating this expression twice yields

$$\begin{aligned} D_{HP}[HP] + D_{P^-}[P^-] &= D_{HP}([HP] + \gamma_{HP}[P^-]) \\ &= D_{HP}[HP]_T \\ &= C_1 + C_2/r \end{aligned} \quad (30)$$

We now define the "dynamic total concentration" of polymer as

$$[HP]_T = [HP] + \gamma_{HP}[P^-] \quad (31)$$

where $\gamma_{HP} = D_{P^-}/D_{HP}$.

Appropriate combinations of the mass balance equations for drug and buffer are

$$\begin{aligned} D_{HA}[HA] + D_{A^-}[A^-] &= D_{HA}([HA] + \gamma_{HA}[A^-]) \\ &= D_{HA}[HA]_T \\ &= C_3 + C_4/r \end{aligned} \quad (32)$$

$$\begin{aligned} D'_{HA}[HA]' + D'_{A^-}[A^-]' &= D'_{HA}([HA]' + \gamma_{HA}[A^-]') \\ &= D'_{HA}[HA]'_T \\ &= C'_3 + C'_4/r \end{aligned} \quad (33)$$

$$\begin{aligned} D_{HB}[HB] + D_{B^-}[B^-] &= D_{HB}([HB] + \gamma_{HB}[B^-]) \\ &= D_{HB}[HB]_T \\ &= C_5 + C_6/r \end{aligned} \quad (34)$$

$$\begin{aligned} D'_{HB}[HB]' + D'_{B^-}[B^-]' &= D'_{HB}([HB]' + \gamma_{HB}[B^-]') \\ &= D'_{HB}[HB]'_T \\ &= C'_5 + C'_6/r \end{aligned} \quad (35)$$

$$\begin{aligned} D_{H^+}[H^+] - D_{OH^-}[OH^-] - D_{A^-}[A^-] - D_{B^-}[B^-] \\ - D_{P^-}[P^-] \\ = C_7 + C_8/r \end{aligned} \quad (36)$$

$$\begin{aligned} D'_{H^+}[H^+]' - D'_{OH^-}[OH^-]' - D'_{A^-}[A^-]' - D'_{B^-}[B^-]' \\ - D'_{P^-}[P^-]' \\ = C'_7 + C'_8/r \end{aligned} \quad (37)$$

Here $C_1, C_2, \ldots, C_8$ are the integration constants, and the dynamic total concentrations are defined as

$$[HY]_T = [HY] + \gamma_{HY}[Y^-] \quad (38)$$

where $\gamma_{HY} = D_{Y^-}/D_{HY}$, and Y may be A^-, B^-, or P^-.

By applying boundary conditions we can evaluate the constants of integration. They are

$$C_1 = D_{HP}[HP]_{T,b}\left(1 + \frac{R}{\delta}\right) - D_{HP}[HP]_{T,p}\frac{R}{\delta} \quad (39)$$

$$C_2 = D_{HP}([HP]_{T,p} - [HP]_{T,b})R\left(\frac{R}{\delta} + 1\right) \quad (40)$$

$$C_3 = D_{HA}[HA]_{T,b}\left(1 + \frac{R}{\delta}\right) - D_{HA}[HA]_{T,p}\frac{R}{\delta} \quad (41)$$

$$C_4 = D_{HA}([HA]_{T,p} - [HA]_{T,b})R\left(\frac{R}{\delta} + 1\right) \quad (42)$$

$$C_4' = qC_4 \quad (43)$$

$$C_5 = D_{HB}[HB]_{T,b} \quad (44)$$

$$C_5' = qC_5 \quad (45)$$

$$C_6 = C_6' = 0 \quad (46)$$

$$C_7 = D_{H+}[H^+]_b - D_{OH-}[OH^-]_b - D_{A-}[A^-]_b - D_{B-}[B^-]_b - D_{P-}[P^-]_b \quad (47)$$

$$C_7' = qC_7 \quad (48)$$

$$C_8 = C_8' = 0 \quad (49)$$

where q is the diffusivity ratio D_i/D_i'. The ratio q is assumed to be the same for all components, since this ratio represents the magnitude of the diffusional pathway changes due to porosity and the tortuosity in the polymer matrix.

The constants of integration are important later on: C_2 and C_4 are used to evaluate J_{HP} and J_{HA}, respectively; C_7 and C_8 are used to evaluate the pH at the polymer/diffusion layer interface; and C_7' and C_8' are used to evaluate the pH at the drug/polymer layer interface.

Determination of Concentrations at the Drug Surface

The pH at the drug surface is crucial, as it determines the concentration of all the other species via the equilibrium relations. At the surface we assume that the concentrations of HA and HP are their intrinsic solubilities. Once the surface pH is known, the other concentrations can be calculated as follows:

$$[A^-]_s = \frac{K_a[HA]_s}{[H^+]_s} = \frac{K_a[HA]_0}{[H^+]_s} \quad (50)$$

$$[P^-]_s = \frac{K_p[HP]_s}{[H^+]_s} = \frac{K_p[HP]_0}{[H^+]_s} \quad (51)$$

$$[OH^-]_s = \frac{K_w}{[H^+]_s} \quad (52)$$

$$[B^-]_s = \frac{K_b[HB]_{T,b}}{\gamma_{HB}K_b + [H^+]_s} \quad (53)$$

In Eq. (53) we have used the definition of the dynamic total solubility to obtain the expressions for $[B^-]_s$. The terms K_p in Eq. (51) and K_b in Eq. (53) refer to the acid dissociation constants of the polymer and buffer, respectively, and they are used to distinguish them from the K_a of the drug.

Using the equilibrium relationships in Eq. (36) along with integration constants C_7' and C_8', we obtain

$$D_{H+}'[H^+]_s - D_{OH-}'\frac{K_w}{[H^+]_s} - D_{A-}'\frac{K_a[HA]_0}{[H^+]_s} - D_{B-}'\frac{K_b[HB]_{T,b}}{\gamma_{HB}K_b + [H^+]_s} - D_{P-}'\frac{K_p[HP]_0}{[H^+]_s} = D_{H+}'[H^+]_b - D_{OH-}'[OH^-]_b - D_{A-}'[A^-]_b - D_{B-}'[B^-]_b D_{P-}'[P^-]_b \quad (54)$$

After rearrangement we get a cubic equation for $[H^+]_s$ that has the standard solution

$$[H^+]_s = 2\sqrt{(-Q)}\cos(\theta/3) - a/3 \quad (55)$$

with

$$\begin{aligned} Q &= (3b - a^2)/9 \\ R &= (9ab - 27c - 2a^3)/54 \\ \theta &= \cos^{-1}(R/\sqrt{Q^3}) \\ a &= \gamma_{HB}K_b - G \\ b &= -(\gamma_1 K_w + \gamma_2 K_a[HA]_0 + \gamma_3[HB]_{T,b} + \gamma_4 K_p[HP]_0 + \gamma_{HB}GK_b) \\ c &= -(\gamma_1 K_w + \gamma_2 K_a[HA]_0 + \gamma_4 K_p[HP]_0)\gamma_{HB}K_b \\ G &= [H^+]_b - \gamma_1[OH^-]_b - \gamma_2[A^-]_b - \gamma_3[B^-]_b - \gamma_4[P^-]_b \end{aligned} \quad (56)$$

where $\gamma_1 = D_{OH-}'/D_{H+}'$, $\gamma_2 = D_{A-}'/D_{H+}'$, $\gamma_3 = D_{B-}'/D_{H+}'$, and $\gamma_4 = D_{P-}'/D_{H+}'$ are ratios of diffusion coefficients. The concentrations at the drug surface are then obtained from the equilibium relationships given above, Eqs. (50)–(53).

Determination of Concentrations at the Polymer/Diffusion Layer Interface

In an analogous fashion we can now obtain the concentrations at the polymer/diffusion layer interface. The polymer concentration, $[HP]_p$, is equal to its intrinsic solubility, $[HP]_0$. The equilibrium relationships at the polymer surface are, after the introduction of the dynamic total solubilities,

$$[A^-]_p = \frac{K_a[HA]_{T,p}}{[H^+]_p + \gamma_{HA}K_a} \quad (57)$$

$$[B^-]_p = \frac{K_b[HB]_{T,p}}{[H^+]_p + \gamma_{HB}K_b} = \frac{K_b[HB]_{T,b}}{[H^+]_p + \gamma_{HB}K_b} \quad (58)$$

For $[P^-]_p$ we use

$$[P^-]_p = \frac{K_p[HP]_p}{[H^+]_p} = \frac{K_p[HP]_0}{[H^+]_p} \quad (59)$$

with

$$[HA]_{T,p} = \frac{[HA]_{T,s} - \alpha[HA]_{T,b}}{\alpha + 1} \quad (60)$$

The parameter α is defined as

$$\alpha = q\frac{R - R_1}{\delta} = q\frac{h}{\delta} \quad (61)$$

Note that α will change during the course of dissolution.

Substituting the above equilibrium relations into Eq. (37) along with the integration constants C_7 and C_8, we obtain

$$D_{H^+}[H^+]_p - D_{OH^-}\frac{K_w}{[H^+]_p} - D_{A^-}\frac{K_a[HA]_{T,p}}{[H^+]_p + \gamma_{HA}K_a} - D_{B^-}\frac{K_b[HB]_{T,b}}{[H^+]_p + \gamma_{HB}K_B} - D_{P^-}\frac{K_p[HP]_0}{[H^+]_P} = D_{H^+}[H^+]_b - D_{OH^-}[OH^-]_b - D_{A^-}[A^-]_b - D_{B^-}[B^-]_b - D_{P^-}[P^-]_b \quad (62)$$

After rearrangement we obtain a quartic equation for $[H^+]_p$:

$$[H^+]_p^4 + a[H^+]_p^3 + b[H^+]_p^2 + c[H^+]_p + d = 0 \quad (63)$$

with

$$\begin{aligned} a &= \gamma_{HA}K_a + \gamma_{HB}K_b - G \\ b &= -[\gamma_1 K_w + G(\gamma_{HA}K_a + \gamma_{HB}K_b) + r_1 + r_2 + r_3 - \gamma_{HA}\gamma_{HB}K_aK_b] \\ c &= -\{r_1(K_p + K_b) + r_2(K_a + K_p) + r_3(K_a + K_b) + \gamma_2 K_w(K_a + K_b + K_p) + G[K_a(K_b + K_p) + K_pK_b] - K_aK_bK_p\} \\ d &= -K_aK_b(\gamma_1 K_w + r_3)\gamma_{HA}\gamma_{HB} \\ G &= [H^+]_b - \gamma_1[OH^-]_b - \gamma_2[A^-]_b - \gamma_3[B^-]_b - \gamma_4[P^-]_b \\ r_1 &= \gamma_2 K_a[HA]_0 \\ r_2 &= \gamma_3[HB]_{T,b} \\ r_3 &= \gamma_4 K_p[HP]_0 \end{aligned} \quad (64)$$

where $\gamma_1 = D_{OH^-}/D_{H^+}$, $\gamma_2 = D_{A^-}/D_{H^+}$, $\gamma_3 = D_{B^-}/D_{H^+}$, and $\gamma_4 = D_{P^-}/D_{H^+}$ are diffusion coefficient ratios. The roots of the quartic equation must be obtained numerically.

Polymer Dissolution and Drug Release Rate

We can derive a simple expression for the dissolution rate of the polymer. First we calculate the derivatives $d[P^-]'/dr$ and $d[P^-]/dr$ at the polymer/diffusion layer interface. The concentration of $[P^-]'$ is calculated from the equilibrium relationship:

$$[P^-]' = K_p\frac{[HP]'}{[H^+]'} \quad (65)$$

Since $[HP]'$ is constant, we obtain

$$\frac{d[P^-]'}{dr} = K_p\frac{[HP]'}{([H^+]')^2}\left(-\frac{d[H^+]'}{dr}\right) \quad (66)$$

The slope, $d[H^+]/dr$, is always negative ($[H^+]$ is diffusing away from the core, which contains weakly acid drug, to the buffered bulk at a higher pH). Also, $d[P^-]/dr$ cannot be positive (for diffusion from the polymer surface) and, furthermore, should be related to $d[P^-]'/dr$ by the appropriate boundary condition (continuity requirement). Hence the only possible condition at the polymer/diffusion layer interface is that

$$\text{at } r = R, \frac{d[P^-]'}{dr} = \frac{d[P^-]}{dr} = 0 \quad (67)$$

This result can now be used to calculate the dissolution rate of the polymer.

$$\begin{aligned} J_{HP} &= -D_{HP}\left(\frac{d[HP]}{dr}\right)_{r=R} = -D_{HP}\left(\frac{d[HP]_T - \gamma_{HP}[P^-]}{dr}\right)_{r=R} \\ &= -\left[\frac{d(C_1 + C_2/r)}{dr}\right]_{r=R} = C_2/R^2 \\ &= \frac{D_{HP}}{\delta}([HP]_{T,p} - [HP]_{T,b})\left(1 + \frac{\delta}{R}\right) \end{aligned} \quad (68)$$

In most cases $\delta \ll R$ and the term $(1 + \delta/R)$ becomes approximately unity and we obtain

$$J_{HP} = \frac{D_{HP}}{\delta}([HP]_{T,p} - [HP]_{T,b}) \quad (69)$$

The value for $[HP]_{T,p}$ is calculated using the pH at the polymer/diffusion layer interface.

The drug release rate J_{HA} can be calculated in a similar fashion:

$$\begin{aligned} J_{HA} &= -D'_{HA}\left(\frac{d[HA]'}{dr}\right)_{r=R_1} \\ &= -D'_{HA}\left(\frac{d[HA]'_T - \gamma_{HA}[A^-]'}{dr}\right)_{r=R_1} \\ &= C'_4/R_1^2 = qC_4/R_1^2 \\ &= \frac{D_{HA}}{\delta}([HA]_{T,p} - [HA]_{T,b})\left(1 + \frac{\delta}{R_1}\right) \end{aligned} \quad (70)$$

In most cases $\delta \ll R_1$ and the term $(1 + \delta/R_1)$ becomes approximately unity and we obtain

$$J_{HA} = \frac{D_{HA}}{\delta}([HA]_{T,p} - [HA]_{T,b}) \quad (71)$$

Time for Onset of Disintegration

We now substitute the expression for dissolution rate of polymer, Eq. (69), into the moving boundary equation, Eq. (4). The resulting expression can be integrated to give the thickness of the polymer as a function of time.

Under sink conditions, $[HP]_{T,b} = 0$, the result is

$$\rho_M\frac{dR}{dt} = -k_s[HP]_{T,p} \quad (72)$$

where $k_s = D_{HP}/\delta$ is the mass transfer coefficient for the polymer. Integration between $t = 0$ ($R = R_2$) and $t = t$($R = R$) gives

$$\rho_M\int_{R_2}^{R}\frac{dR}{[HP]_{T,p}} = -k_s\int_0^t dt \quad (73)$$

or

$$t = \frac{\rho_M}{k_s}\int_R^{R_2}\frac{dR}{[HP]_{T,p}} \quad (74)$$

This integration is performed numerically since $[HP]_{T,p}$ depends on R, Eqs. (60) and (61). Scanning electron microscopy indicates (see Results) that the coating is still intact after 90% of the coating has dissolved. We thus choose to approximate the time for onset of disintegration to correspond to the time at which a 95% reduction in the polymer thickness has occurred, that is, when the upper limit on the integral is

$$R = R_1 + 0.05(R_2 - R_1) \quad (75)$$

Table I. Formulations of PVAP-Coated Tablets (Quantities Are Given as Weight Percentage)

Formulation					
Placebo		Buffer		Aspirin	
Starch 1500	49.75	Avicel 101	18.8	Aspirin	90
Avicel 101	49.75	Stearic acid NF	1.0	Avicel 101	9
Fumed silica NF	0.25	Talc 140	1.0	Ac Di Sol	1
Magnesium stearate	0.25	Croscarmellose Sodium NF	4.0		
		Sodium citrate dihydrate	25.07		
		Disodium citrate	50.13		

MATERIALS AND METHODS

Tablets

Three batches of PVAP-coated tablets were prepared to investigate the effect of the core pH on the coating dissolution time. The first of these batches contained a placebo formulation, the second contained aspirin to generate an acidic core, and the third contained citrate salts to maintain a core pH of pH 6.5. Individual formulations are given in Table I. All three batches were coated with PVAP from an aqueous-based pseudolatex dispersion (Colorcon Inc., West Point, Pa.) in a side-vented pan apparatus (24-in. Accelacota, Thomas Eng., Hoffman Est., Ill.) using identical operating conditions. Polyethylene glycol was used as the plasticizer, and no pigments were added to the coating dispersion. The batch size was 10 kg in each case.

Disintegration Test

The USP test procedure was modified to omit the placement of disks in the tubes and by using 0.05 *M* phosphate buffers in lieu of simulated intestinal fluid USP so that disintegration could be studied as a function of pH over the range pH 5.5 to 6.8. For the purpose of this study, we defined the onset of disintegration as the time when the coating is first ruptured. This was done to circumvent any artifactual differences arising from variation in the disintegration time among the three tablet core formulations.

Scanning Electron Microscopy (SEM)

PVAP-coated tablets that had been subjected to dissolution testing in either simulated gastric fluid USP (without pepsin) or simulated intestinal fluid USP (without bile salts) for 1 h at 50 rpm and 37°C in a USP basket dissolution apparatus were allowed to dry and then submitted for scanning electron microscopy along with control tablets from the same batch. Note that under the test conditions applied the coatings remained intact for the duration of the dissolution experiment. SEM samples were prepared by cutting the tablets in a vertical cross section or by directly observing the coating surface. In either case, the sample was attached to the mounting with double-sided tape and colloidal graphite, then coated with approximately 15 nm gold/palladium in an E50-100 sputter coater (Polaron, Hatfield, Pa.). The sample was then studied in an ISI-DS 130 SEM (International Scientific Instruments Inc., Milpitas, Calif.) at a pressure of approximately 10^{-6} Torr and at magnifications ranging from 60× to 3500×.

PVAP Dissolution Tests

The dissolution rate of PVAP as a function of pH was measured in a rotating disk apparatus at 200 rpm. The pH was controlled by a pH stat method for unbuffered media or by the use of 0.05 *M* phosphate buffer. Complete details of the experimental apparatus have been described by McNamara and Amidon (16). The absorbance of the dissolution medium at 230 nm was monitored continuously using a flow-through cell in a Lambda 3 UV–vis spectrophotometer (Perkin–Elmer, Oak Brook, Ill.). The dissolution rate was then calculated using the absorptivity at pH 6.8 (α = 20.04).

Statistical Analysis

All results presented for disintegration tests represent the means and standard deviations calculated from a sample of $N = 6$ except where specifically noted. Analysis of variance was used to evaluate the effect of changing the core composition. For the dissolution of PVAP, linear regression analysis was used to determine the slope of the absorbance versus time plot.

RESULTS AND DISCUSSION

Based on the model presented, numerical solutions were used to predict concentration profiles of the polymer and drug and the pH profile in the coating and aqueous boundary layers. The rate of polymer dissolution and release of drug prior to the onset of disintegration was also simulated, and predictions were obtained for the time of onset of core disintegration. The predicted behavior was then compared with experimental data to evaluate to what extent the model could predict the observed behavior and to identify any problems with assumptions made in setting up the model. Experimental data included SEM and determining changes in release rate with buffer strength and stirring rate in the dissolution medium. In addition, the effect of changing the pH of the core material relative to the medium pH on the disintegration time was investigated. After establishing that the model predicts a satisfactory description of

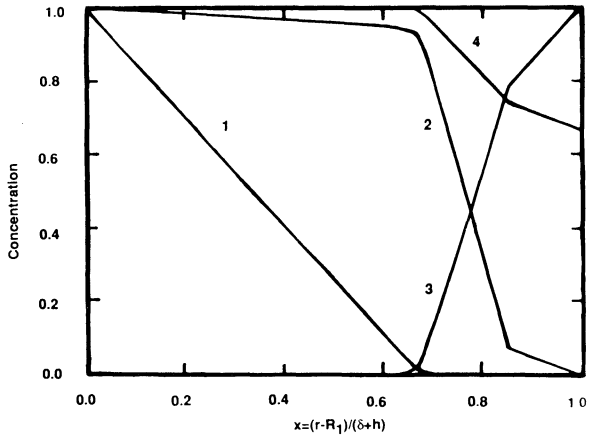

Fig. 3. Fractional concentration profiles with the fractional dimensionless distance for enteric-coated aspirin in a phosphate buffer solution with pH_b = 6.8. Parameters used are as follows: polymer acidity, pK_p = 4.5; solubility, $[HP]_0 = 5 \cdot 10^{-6}$ *M*; α = 58.6; $\gamma_1 = \gamma_2 = \gamma_3$ = 0.2; and diffusivity ratio, q = 10. 1, HA; 2, A^-; 3, $[B^-]$; 4, [HB].

experimental dissolution and disintegration data, its application to the design of enteric-coated tablets is discussed.

Simulated Concentration Profiles

Figure 3 represents the concentration profiles in the dissolving coating region and aqueous boundary layer (see Appendix B) for a polymer of pK_p = 4.5 (pK_p is used throughout for the polymer dissociation constant to distinguish it from that of the drug, pK_a). Values chosen are illustrative for a low-pK_a polymer having a solubility similar to that of PVAP. The polymer surface in this example is located at $x = (r - R_1)/(h + \delta) = 0.85$, i.e., 85% of the region of interest is the polymer coating, with the remaining 15% occupied by the stagnant diffusion layer. At the interface of the polymer and the stagnant diffusion layer the concentration profile of each species changes curvature due to the different diffusivities in the two regions. All species are considered to diffuse through aqueous pores in the coating layer, but the diffusivity is altered by the porosity and tortuosity of the polymer, resulting in a reduced apparent diffusivity, D_i', for each species. The short lag time observed between the immersion of the dosage form and the appearance of aspirin in the dissolution medium is consistent with aqueous pore diffusion rather than a solution/diffusion mechanism. Since all buffer and drug species are small, the ratios of their diffusivities in the polymer versus stagnant diffusion layer, q, are assumed to be the same. Because of the tortuosity of the aqueous pores in the hydrated polymer layer, q values of greater than unity are expected.

Figure 4 illustrates pH profiles in the coating and stagnant diffusion layer for the case of an enteric-coated aspirin dosage form with polymer pK_p = 4.5. For diffusivity ratio, q, values of 5 or greater, the pH profile becomes relatively insensitive to the q value. In subsequent simulations a q value of 10 is used.

The dynamics of the polymer erosion and drug release are presented in Fig. 5. The time is scaled to the time at which the coating dissolution is 95% complete, which is assumed to coincide with the rupture of the coating and the onset of tablet disintegration. Initially, the polymer dissolves quickly. As the polymer layer thins, the resistance to drug transport decreases and so the drug is released faster. Meanwhile, the increase in concentration of acidic drug in the coating layer results in a reduction in pH, and this in turn leads to a reduction in the polymer dissolution rate. Overall, the dissolution rate of the polymer decreases with time, while the release rate of the drug increases with time. Implicit to the model and these results is the assumption that the polymer dissolution occurs at the polymer/bulk interface. This assumption was tested by subjecting tablets to simulated gastric and intestinal dissolution media, then studying them by SEM.

Scanning Electron Microscopy

To investigate changes in the polymer layer under different dissolution conditions, scanning electron microscopy (SEM) was run on three types of samples: control tablets, tablets subjected to dissolution testing under simulated gastric conditions, and tablets subjected to testing under simulated intestinal conditions. Representative micrographs are shown in Fig. 6. Controls had smooth coating surfaces and the cross-section SEM indicated that the coating thickness was approximately 150 μm. After treatment in simulated gastric conditions, the smooth appearance of the coating surface (Fig. 6A) was retained. Cross section (Fig. 6B) indicated that a minimal amount of polymer had dissolved, at most 10%. There was some water penetration into the core, as evidenced by an alteration in the appearance of the aspirin crystals (note: Fig. 6C is of a section that showed the most change in morphology from the control). Any release during the acid phase (up to 3% release in 1 h at 50 rpm) can be accounted for by dissolution of aspirin in the water penetrating to the core surface and subsequent diffusion out through the hydrated polymer phase. After treatment in simulated intestinal intestinal conditions, the coating developed

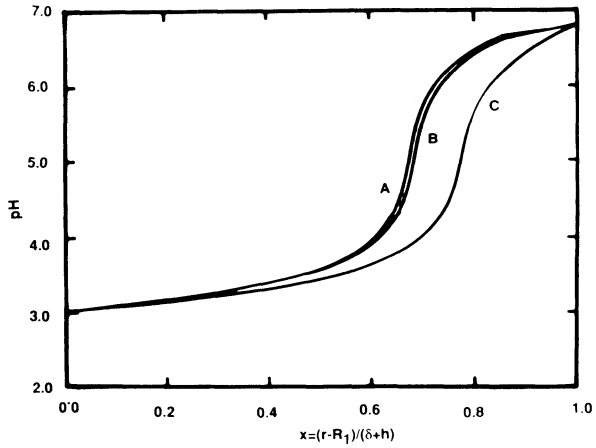

Fig. 4. The effect of the diffusivity ratio, q, on the pH profile in enteric-coated aspirin in a phosphate buffer. Apart from the diffusivity ratio the same parameters given in the legend to Fig. 2 are used. (A) q = 10; (B) q = 5; (C) q = 2

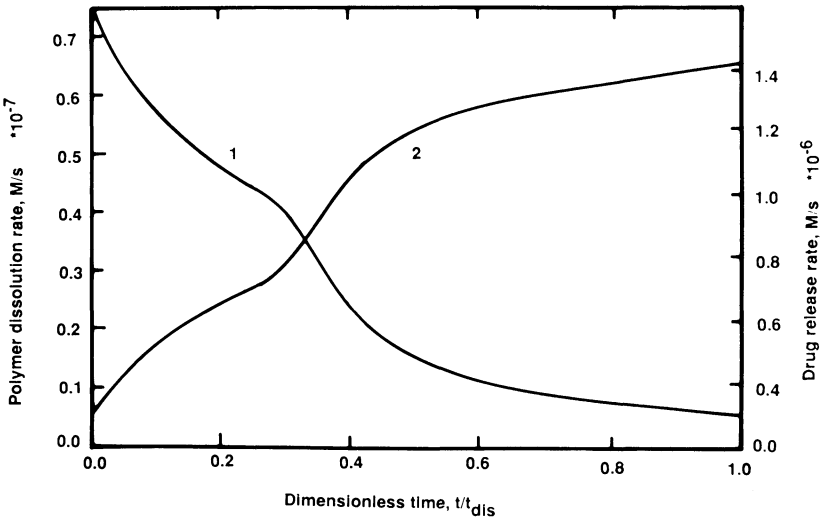

Fig. 5. Dissolution rate of polymer (line 1) and release rate of drug (line 2) during the course of disintegration.

a roughened appearance on the surface (Fig. 6D). On viewing the cross section (Fig. 6E), it was apparent that the majority of the polymer, approximately 90% by comparison with the original coating thickness, had dissolved. The greater release of aspirin under simulated intestinal conditions as compared to the simulated gastric phase can be accounted for by the reduction in the thickness of polymer through which the aspirin must diffuse (note that at 50 rpm, the coating remained intact over the 1-hr duration of both the simulated gastric and the intestinal dissolution experiments). From the cross-section micrograph one can also observe that there was more substantial drug dissolution in the core during exposure to simulated intestinal conditions—the morphology of the core material was substantially different from that of the control or gastric-phase tablets (again, Fig. 6F is of a section which showed maximal change in morphology from the control).

SEM studies therefore validated the assumption that polymer dissolution occurs primarily at the polymer/bulk interface rather than by bulk erosion throughout the coating layer. Also, SEM measurements indicated that over 90% of the coating dissolves prior to the onset of the core disintegration. This result formed the basis for our assumption that the time for onset of disintegration occurs at approximately 95% coating dissolution.

However, the alteration in the morphology of the core material during the polymer dissolution phase suggests that the assumption of zero flux of species other than HA at the core/polymer interface is useful only as an approximation, rather than providing a precise physical description of the conditions at the interface. The model assumes that the core consists of solid, compacted drug but in the real situation the excipients in the core formulation modify the behavior at the core/polymer interface. The effect of water flux into the tablet would be to create a larger surface area for drug dissolution and hence a faster dissolution rate. However, the concentration of drug at the core/polymer interface would still be limited by the drug's solubility. Provided that the volume of water imbibed and drug solubility are low, the driving force for drug release, i.e., the concentration at the drug/polymer interface, will still be the drug solubility and hence invariant. Further, provided that the influx of water is small, there will be little influx of buffer species and so the pH calculated for the surface of the core will still be reasonably accurate. The net effect of water influx to the core will be to increase the rate of polymer dissolution and drug release, so the model predictions for the rate of release and time for onset of core disintegration may underestimate the observed release rate.

Bulk and Core pH

Figure 7 shows the predicted pH profile in the coating layer when an acidic drug is added to the core formulation. The presence of an acidic drug, in this case aspirin, in the tablet core is predicted to result in a lowering of the pH in the coating layer relative to that of the bulk. For aspirin, the pH at the surface is predicted to be pH 3. The pH at the polymer/boundary layer interface depends on the diffusivity ratio, q, as well as the bulk and surface pH. For a bulk pH of 6.8 and core surface pH of 3, the pH at the polymer/boundary layer interface falls in the range of pH 6.2 to 6.6 at reasonable values of q.

The concentration profile of ionized polymer has a maximum at the polymer/boundary layer interface. This occurs because the ratio of $[H^+]$ to polymer concentration differs in the two regions. Near the tablet surface, $[H^+]$ is high, suppressing the ionization of polymer. Close to the polymer/boundary layer interface, $[H^+]$ decreases and ionization of polymer (reaction ϕ_3) proceeds, leading to an increase in $[P^-]$. In the boundary layer, P^- is diffusing across a concentration gradient (assuming sink conditions in the bulk), leading to a decrease in concentration with distance.

The effect of the bulk and core pH on the disintegration time of PVAP-coated tablets is shown in Fig. 8. In the case of placebo cores, the disintegration time progressively decreases above pH 5. This may be expected, since the polymer has a pK_a of 4.7. When aspirin (pK_a 3.5) is incorpo-

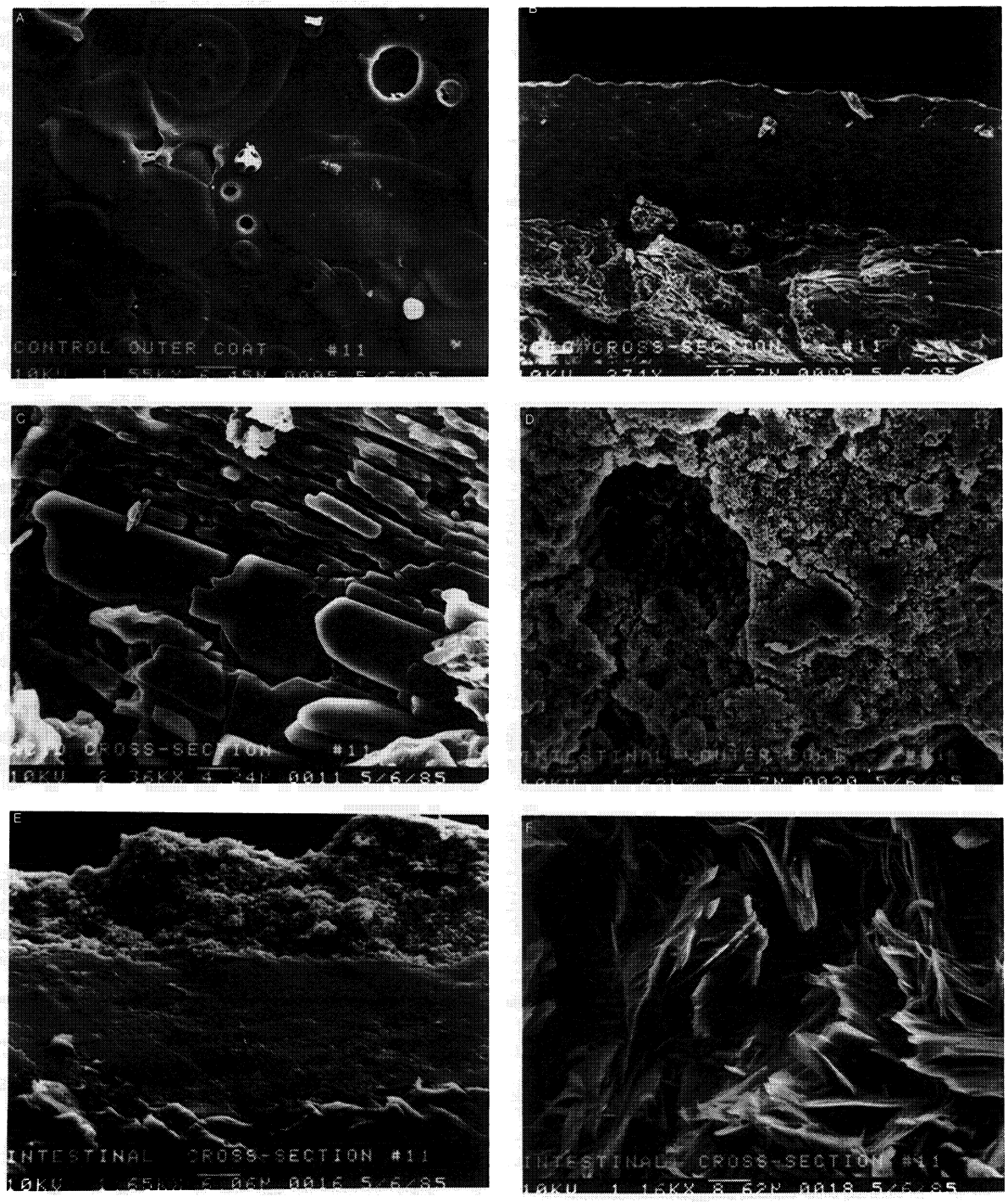

Fig. 6. Scanning electron micrographs of PVAP-coated tablets subjected to simulated gastric or intestinal conditions. (A) Coating surface after simulated gastric conditions; (B) coating cross section (gastric); (C) core cross section (gastric); (D) coating surface after simulated intestinal conditions; (E) coating cross section (intestinal); (F) core cross section (intestinal).

rated in the core, dissolution is very slow at pH 5 and there is a shift in the pH/disintegration profile to disintegration at higher pH values. There is a steep dependency in the pH range 5.5 to 7.0 even though the pK_a of the polymer is substantially below this range. These results are predicted well by the model and reflect the ability of the aspirin to buffer the coating layer even in the presence of buffer diffusing in from the bulk. Additionally, when citrate is incorporated in the core, the dependency of disintegration time on bulk pH in the pH range 5 to 7 is virtually eliminated, with rapid disintegration occurring over the whole range. This effect is also consistent with the model, which predicts that the core pH will affect the pH profile in the coating layer and hence the dissolution rate of the polymer.

The current data are also consistent with data obtained previously by Dressman and Amidon (17). In those experi-

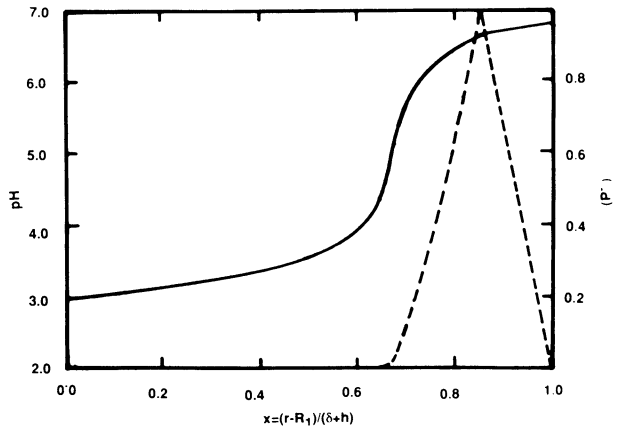

Fig. 7. pH (solid line) and [P^-] (dashed line) profiles with the fractional dimensionless distance for enteric-coated aspirin in a 0.05 *M* phosphate buffer solution with pH_b = 6.8.

ments, three batches of tablets were made in which the core pH was adjusted between pH 3 and pH 5. All three batches were coated with hydroxypropylmethylcellulose phthalate. A core pH of 5 resulted in a significant decrease in the *in vivo* disintegration time compared to those with a core pH of pH 3.

The great dependency of coating dissolution on the bulk pH when acidic or nonionizing compounds form the core material suggests that it is critical to the prediction of *in vivo* performance to choose a pH that is representative of conditions in the proximal small intestine. Previous data (18) suggest that the fasting pH is about 5.5 to 6.0 in healthy young adults and that factors such as meal intake (19), age (20), and disease state (21) can affect the local pH.

Buffer Concentration

The effects of buffer concentration, a further determinant of the pH profile in the polymer layer, are shown in Fig. 9. Disintegration time is predicted as a function of buffer concentration for different bulk pH values. At very low buffer concentrations, the prime determinant of the [H^+] profile in the polymer layer is the H^+ generated by the dissolving drug, resulting in long predicted disintegration times. At a bulk pH of 6.5, a small increase in the buffer concentration results in a large decrease in the disintegration time, and at concentrations in excess of 0.05 *M* the disintegration time is short and practically independent of further increases in the buffer concentration. At pH 6, more typical of fasting-state pH in the upper small intestine, the decrease in disintegration time with increases in buffer concentration is predicted to be much more gradual, with a fourfold change in disintegration time over the concentration range 0.02 to 0.1 *M*, a range typical of buffers used as dissolution media. At pH 5.5, a lower-limit estimate of fasted pH in the duodenum but fairly typical of fed-state upper intestinal pH, disintegration is predicted to be longer and less sensitive to changes in the buffer concentration. Note that the concentration and pH range over which the disintegration time is very sensitive to buffer concentration depends on the polymer pK_p and that the simulations discussed here refer to a pK_p of 4.5.

In vitro data collected for aspirin release from PVAP-coated aspirin tablets as a function of buffer concentration (see Fig. 10) support the predicted behavior. As the buffer concentration is increased from 0.05 to 0.1 *M*, the percentage of aspirin released in 1 hr of dissolution testing in phosphate buffer increased by a factor of 10. No direct comparison between predicted and observed behavior can be made, because at higher buffer concentrations, polymer dissolution was complete within 1 hr and the tablets disintegrated, thereby changing the mechanism of aspirin release (from diffusion through the coating to direct dissolution from the core material).

In an attempt to ascertain how well the buffer capacity of simulated intestinal fluid at pH 6.8 simulates the buffer capacity in the gut, we fed two dogs with midgut fistulae regular dog food meals and collected chyme in 25-ml

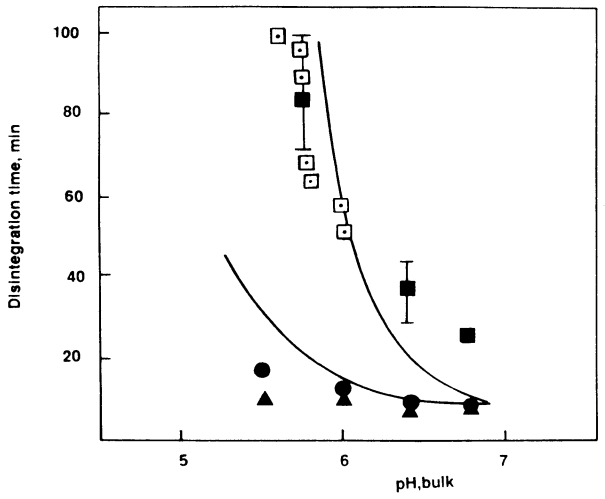

Fig. 8. Simulated (lines) and experimental data for time of onset of disintegration of PVAP-coated aspirin (■), placebo (●), and citrate (▲) tablets, as a function of bulk pH. Open squares represent individual data; filled symbols are the means of six values. Error bars represent standard deviations; in most cases these were smaller than the symbol size.

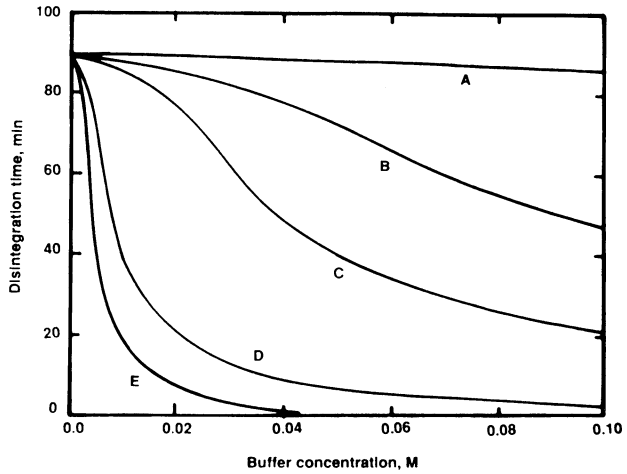

Fig. 9. Model predictions for the effect of buffer concentration (pK_b = 7.1) on disintegration time for aspirin tablets coated with a polymer of pK_p = 4.5. (A) pH_b = 5; (B) pH_b = 5.5; (C) pH_b = 6; (D) pH_b = 6.5; (E) pH_b = 7.

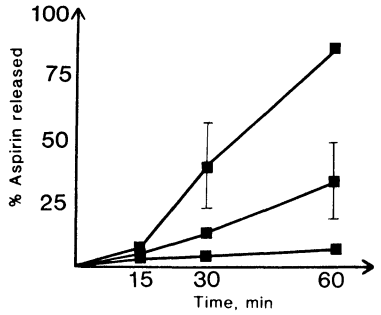

Fig. 10. Percentage aspirin released from PVAP-coated tablets as a function of time at a stirring rate of 100 rpm in 0.025 *M* (lower curve), 0.05 *M* (middle curve), and 0.10 *M* (upper curve) phosphate buffer at pH 6.8.

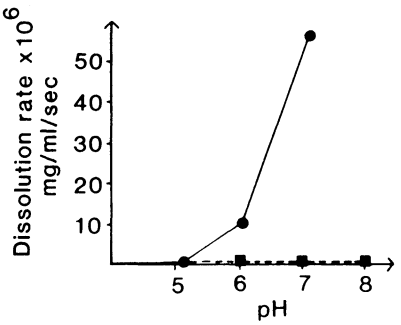

Fig. 11. Dissolution of PVAP in rotating disk apparatus using unbuffered medium (squares) and 0.05 *M* phosphate buffer (circles) as a function of pH.

samples early, in the middle, and late in the postprandial phase. We then measured the pH of the chyme sample and titrated to a 1-pH unit change with 0.1 *N* HCl. The buffer capacity was calculated as milliequivalents per liter per pH unit. Simulated intestinal fluid without pancreatin was similarly titrated. The results are shown in Table II.

The pH of the simulated fluid is a good representation of the postprandial midgut pH in dogs, a fair representation of the fasted intestinal pH in humans (pH 5.5 to 6.5), and substantially higher than the postprandial intestinal pH in humans. The buffer capacity is somewhat lower than that of the mid-to-late chyme collections. Since the concentration of the buffer in the simulated fluid falls in a region of the disintegration time versus buffer concentration plot that appears to be quite sensitive to changes in intestinal pH, it seems that closer attention needs to be paid to the comparison of dissolution and disintegration media in terms of buffer capacity, so that *in vitro* results will more closely predict those obtained *in vivo*.

To test whether the effect of buffer concentration results from the effect on the polymer dissolution, we also studied the dissolution of the pure polymer in buffered and unbuffered media over a wide pH range. Figure 11 shows that when using a pH stat in the unbuffered mode, the dissolution of PVAP is very slow even at basic pH, whereas in buffered media, dissolution increases rapidly at a pH about 1 pH unit above the pK_a {reported as 4.7 (Colorcon, Inc., based on solubility data (22)] and 4.9 [potentiometric titration (23)]}. These results can be explained by the ability of PVAP to suppress its own ionization at the unbuffered dissolving surface.

Table II. Buffer Capacity of Chyme at Midgut in Two Fistulated Dogs

Dog No.	Solution	Initial *p*H	Buffer capacity (mEq/liter/*pH* unit)
1	Early chyme	6.75	28
	Mid	6.82	32
	Late	6.88	48
2	Early	6.50	24
	Mid	6.59	35
	Late	6.79	44
SIF		6.8	26

Stirring Rate

The effect of stirring rate in the USP No. 1 apparatus was investigated. Increasing the stirring rate is predicted to decrease the thickness of the aqueous boundary layer, thereby increasing the mass transfer rate. The net effect is a direct relationship between the mass transfer coefficient and the release rate of drug, as shown in Fig. 12. The dependency of the mass transfer coefficient on the stirring rate was predicted by the model to be $k_s \simeq (\text{stirring rate})^{2.5}$. We then measured the dependency experimentally by packing an ion exchange resin (Amberlite 400) into the basket apparatus and measuring the uptake rate of H^+ from an acidic solution (using an Orion pH meter) as a function of stirring rate. The experimentally determined relationship was $k_s = (\text{stirring rate})^{2.47}$, in close agreement with the model prediction. The sensitivity of the mass transfer coefficient to the stirring rate in the basket apparatus suggests that the stirring rate is very important to the outcome of *in vitro* dissolution tests and that, until the effective *in vivo* mass transfer coefficient range can be established, using an inappropriate stirring rate may be a major source of poor correlation between *in vitro* and *in vivo* data.

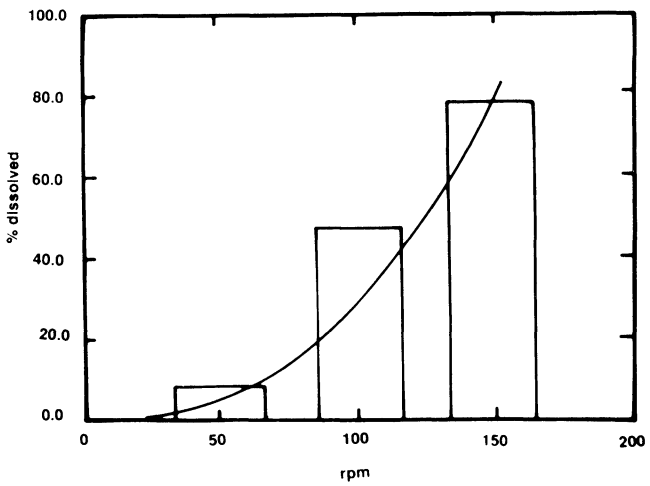

Fig. 12. Effect of stirring rate on percentage aspirin release in 1 hr in rotating basket (USP No. 1) apparatus. A 0.05 *M* phosphate buffer, pH 6.8, was used as the dissolution medium. Bars are experimental data ($N = 6$; coefficients of variation, 14% at 50 rpm, 29% at 100 rpm, and 15% at 150 rpm); the line is the model prediction.

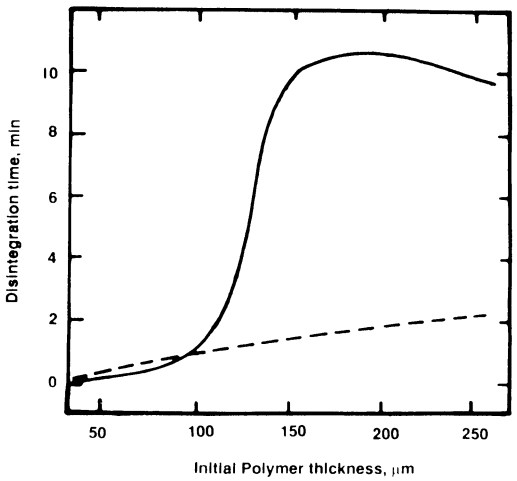

Fig. 13. Model predictions for the effect of initial polymer thickness on disintegration time for tablets with a neutral core (dashed line) and with a weak acid core (e.g., aspirin) (solid line).

Application to Design of Enteric-Coated Dosage Forms

Design of an enteric-coated dosage form with optimal properties in terms of low drug release during gastric residence combined with rapid disintegration at intestinal pH requires consideration of the pH generated at the core surface (drug solubility and pK_a and buffer capacity of the bulk) and polymer pK_a, solubility, and thickness. Other aspects of the formulation, e.g., the disintegrant action, may in some instances provide the rate-limiting step to drug release from the core. However, this is a separate issue that cannot be addressed within the scope of the current model. Bulk buffer effects are dictated by the bicarbonate/chloride buffer environment in the small intestine, which sustains a buffer capacity of about 40 mEq/pH unit, as measured postprandially in mongrel dogs. The buffer capacity of the intestine in humans has not been directly measured as far as we know. Application of this model to design of enteric-coated dosage forms is also limited by the various assumptions made, the most important to quantitative predictability being that disintegration will occur when polymer dissolution is 95% complete, that there is no net flux of species other than HA at the core surface, and that the model strictly applies only for drugs where the core pH generated is lower than that of the polymer pK_a (if the pH generated is much greater than the polymer pK_a, there can be polymer dissolution throughout the coating layer).

Simulations for the effect of the polymer thickness on the disintegration time are shown in Fig. 13, for the case of enteric-coated aspirin and neutral tablets. For neutral cores, a gradual increase in disintegration time with thickness is predicted. In contrast, for aspirin tablets a steep dependency on thickness is predicted between 100- and 200-μm coating, above which there is little dependency. The contrasting profile for aspirin cores occurs because of two opposing trends with increasing thicknesses. At greater thicknesses, there is faster dissolution at the polymer/boundary interface, but there is more total polymer to dissolve.

The effects of changing pK_a and solubility of the drug on the disintegration time in pH 6.8 buffer are simulated in Fig. 14, for a PVAP coating 150 μm thick. For drugs with a low solubility, the disintegration time will be short irrespective of the pK_a, because the buffer capacity of the dissolving drug will be limited by its solubility. The result is similar for high-pK_a acids, as again, the ability to reduce the pH in the coating layer will be minimal. For soluble drugs ($[HA]_0 > 0.5$ *M*) with a pK_a of <5, the disintegration is predicted to be prolonged by the lowering of the pH in the coating layer by the drug. These criteria apply to several drugs that are potential candidates for enteric coating, e.g., agents used to treat urinary tract infections and NSAIDs, some of which are irritating to the gastric mucosa.

Another variable in the formulation is the polymer used for the coating process. Several polymers are used for enteric coating, each having a distinct pK_p and solubility. The effects of polymer properties on the disintegration time are simulated in Fig. 15. Lower intrinsic polymer solubility and higher pK_p are predicted to result in prolonged disintegration times. The choice of polymer will depend on the tablet substrate. For acidic drugs, it may be desirable to offset the pH lowering effect of the drug by choosing a polymer with a lower pK_p, whereas for basic drugs, one may need a higher-pK_p polymer to avoid dosage form disintegration during gastric residence.

Overall, the model is potentially quite useful as a guide to the choice of polymer properties (pK_a, solubility, and thickness) that will optimize the performance of the enteric-coated dosage form.

SUMMARY

In this paper we have presented a model for polymer dissolution and drug release from enteric-coated tablets. It is shown that the dissolution rate and the time of onset of disintegration are dependent on several parameters. These parameters include the medium (K_p and C_b), the drug (pK_a, $[HA]_0$), and the polymer (pK_p, $[HP]_0$, and q) properties and the mass transfer characteristics (D and δ) of the system. The model should be useful in prediction of the drug release during the polymer disintegration phase and also the time of onset of disintegration, for any combination of weakly acidic

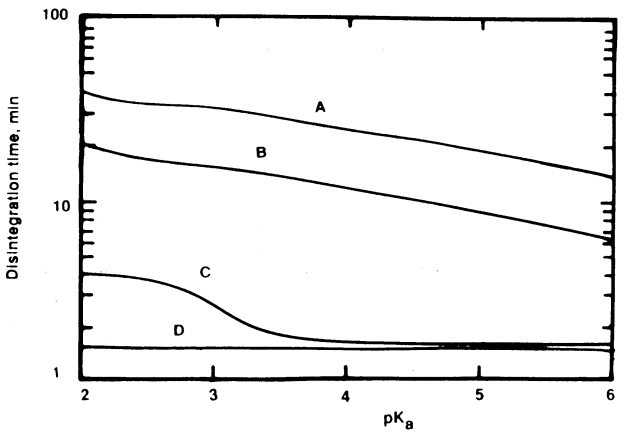

Fig. 14. Model predictions for the effect of drug pK_a and solubility on disintegration time. A, $[HA]_0 = 0.10$ *M;* B, $[HA]_0 = 0.050$ *M;* C, $[HA]_0 = 0.01$ *M;* D, $[HA]_0 = 0.001$ *M*.

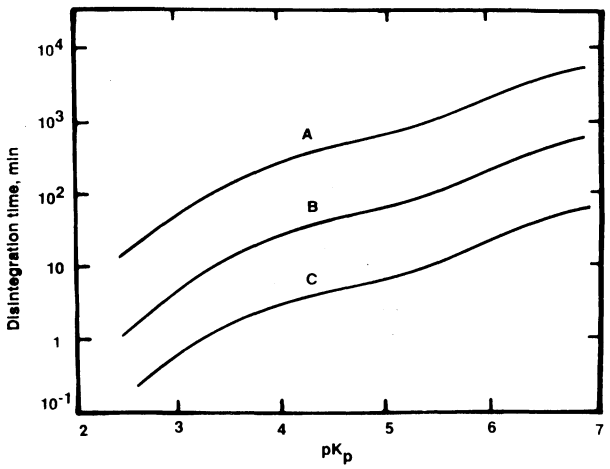

Fig. 15. Model predictions for the effect of polymer solubility and polymer pK_p on disintegration time. A, $[HP]_0 = 10^{-7}$ *M*; B, $[HP]_0 = 10^{-6}$ *M*; C, $[HP]_0 = 10^{-5}$ *M*.

drug and polymer coating, and therefore can be applied to optimizing the formulation of enteric-coated dosage forms. Additionally, it is shown that a range of disintegration times can be obtained by manipulating the buffer pH and concentration and stirring rate in the *in vitro* testing procedure. The relevance of *in vitro* results to *in vivo* performance is contingent upon the appropriate choice of test conditions based on known gastrointestinal physiology.

APPENDIX A. CHARGE BALANCE CONSIDERATIONS

One important requirement that must be fulfilled by the solution to the system equations is the zero-current or "electroneutrality" requirement (24). That corresponds to zero potential and therefore zero flux due to electrostatic forces in the diffusion layer, so that Fick's law for diffusion can be applied. In terms of fluxes the requirement can be stated as (25)

$$\Sigma z_i J_i = 0 \tag{76}$$

where z_i is the charge of the component i and J_i is the molar flux. The equations derived here for the polymer phase and stagnant film satisfy this constraints. The proof is given only for the latter case, however, the same applies for the polymer phase.

In stagnant film Eq. (76) becomes

$$D_{H^+}\frac{d[H^+]}{dr} + D_C\frac{d[C]}{dr} - D_{A^-}\frac{d[A^-]}{dr} - D_{OH^-}\frac{d[OH]^-]}{dr} - D_{P^-}\frac{d[P^-]}{dr} + z_{B^-}D_{B^-}\frac{d[B^-]}{dr} + z_{HB}D_{HB}\frac{d[HB]}{dr} = 0 \tag{77}$$

Here [C] represents the cation concentration. For this last equation an additional boundary condition is, at bulk, $r = R + \delta$:

$$[C] = [C]_b \tag{78}$$

Integration of Eq. (77) between $r = r$ and $r = R + \delta$ (bulk) gives

$$\begin{aligned} D_{H^+}[H^+] + D_C[C] - D_{A^-}[A^-] - D_{OH^-}[OH^-] - D_{P^-}[P^-] \\ + z_{B^-}D_{B^-}[B^-] + z_{HB}D_{HB}[HB] = D_{H^+}[H^+]_b \\ + D_C[C]_b - D_{A^-}[A^-]_b - D_{OH^-}[OH^-]_b \\ - D_{P^-}[P^-]_b + z_{B^-}D_{B^-}[B^-]_b + z_{HB}D_{HB}[HB]_b \end{aligned} \tag{79}$$

Since the cation (C) is not involved in any of the reactions,

$$[C] = [C]_b \tag{80}$$

and from Eq. (34),

$$\begin{aligned} D_{B^-}[B^-] + D_{HB}[HB] &= D_{B^-}[B^-]_b + D_{HB}[HB]_b \\ &= D_{HB}[HB]_{T,b} \end{aligned} \tag{81}$$

Furthermore, noting that $z_{B^-} = z_{BH} - 1$, we get

$$\begin{aligned} D_{H^+}[H^+] - D_{A^-}[A^-] - D_{OH^-}[OH^-] - D_{B^-}[B^-] \\ - D_{P^-}[P^-] = D_{H^+}[H^+]_b - D_{A^-}[A^-]_b \\ - D_{OH^-}[OH^-]_b - D_{B^-}[B^-]_b - D_{P^-}[P^-]_b \end{aligned} \tag{82}$$

which is Eq. (36) with determined integration constants.

APPENDIX B. CONCENTRATION PROFILES

We can evaluate the concentration profiles, since at each point, the equilibrium relationships must hold.

In the $R_1 < r < R$ region (polymer layer) the concentration of the polymer is constant and we have

$$[A^-]' = \frac{K_a[HA]_T}{[H^+]' + \gamma_{HA}K_p} \tag{83}$$

$$[B^-]' = \frac{K_b[HB]_T}{[H^+] + \gamma_{HB}K_b} \tag{84}$$

For $[P^-]'$ we use

$$[P^-]' = \frac{K_p[HP]_s}{[H^+]'} = \frac{K_p[HP]_0}{[H^+]'} \tag{85}$$

Using these expressions in Eq. (37) we can get

$$\begin{aligned} D'_{H^+}[H^+]' - D'_{OH^-}\frac{K_w}{[H^+]'} - D'_{A^-}\frac{K_a[HA]_T}{[H^+]' + \gamma_{HA}K_a} \\ - D'_{B^-}\frac{K_b[HB]_T}{[H^+]' + \gamma_{HB}K_b} - D'_{P^-}\frac{K_p[HP]_0}{[H^+]'} \\ = D'_{H^+}[H^+]_b - D'_{OH^-}[OH^-]_b - D'_{A^-}[A^-]_b \\ - D'_{B^-}[B^-]_b - D'_{P^-}[P^-]_b \end{aligned} \tag{86}$$

After rearrangement a quartic equation for $[H^+]'$ is obtained

$$([H^+]')^4 + a([H^+]')^3 + b([H^+]')^2 + c[H^+]' + d = 0 \tag{87}$$

with

$$\begin{aligned} \alpha &= \gamma_{HA}K_a + \gamma_{HB}K_b - G \\ b &= -[\gamma_1 K_w + G(\gamma_{HA}K_a + \gamma_{HB}K_b) + r_1 + r_2 + r_3 \\ &\quad - \gamma_{HA}\gamma_{HB}K_aK_b] \\ c &= -[r_1\gamma_{HB}K_b + r_2\gamma_{HA}K_a + (\gamma_1 K_w + r_3)(\gamma_{HA}K_a \\ &\quad + \gamma_{HB}K_b) + G\gamma_{HA}\gamma_{HB}K_aK_b] \\ d &= -\gamma_{HA}\gamma_{HB}K_aK_b(\gamma_1 K_w + r_3) \\ G &= [H^+]_b - \gamma_1[OH^-]_b - \gamma_2[A^-]_b - \gamma_3[B^-]_b - \gamma_4[P^-]_b \\ r_1 &= \gamma_2 K_a[HA]_T = \gamma_2 K_a(C'_3 + C'_4/r) \\ r_2 &= \gamma_3[HB]_{T,b}K_b \\ r_3 &= \gamma_4 K_p[HP]_0 \end{aligned} \tag{88}$$

Solution of the quartic equation can be done numerically by the Newton–Raphson method (26).

In the $R < r < R + \delta$ region (diffusion layer) we have

$$[A^-] = \frac{K_a[HA]_T}{[H^+] + \gamma_{HA}K_a} \tag{89}$$

$$[B^-] = \frac{K_b[HB]_T}{[H^+] + \gamma_{HB}K_b} \tag{90}$$

For $[P^-]$ we use

$$[P^-] = \frac{K_p[HP]_T}{[H^+] + \gamma_{HP}K_p} \tag{91}$$

Using these expressions in Eq. (36) we can get

$$\begin{aligned} D_{H^+}[H^+] - D_{OH^-}\frac{K_w}{[H^+]} - D_{A^-}\frac{K_a[HA]_T}{[H^+] + \gamma_{HA}K_a} \\ - D_{B^-}\frac{K_b[HB]_{T,b}}{[H^+] + \gamma_{HB}K_b} - D_{P^-}\frac{K_p[HP]_0}{[H^+] + \gamma_{HP}K_p} \\ = D_{H^+}[H^+]_b - D_{OH^-}[OH^-]_b - D_{A^-}[A^-]_b \\ - D_{B^-}[B^-]_b - D_{P^-}[P^-]_b \end{aligned} \tag{92}$$

After arrangement a fifth-order equation for $[H^+]$ is obtained:

$$[H^+]^5 + a[H^+]^4 + b[H^+]^3 + c[H^+]^2 + d[H^+] + e = 0 \tag{93}$$

with

$$\begin{aligned} a &= \gamma_{HA}K_a + \gamma_{HB}K_b + \gamma_{HP}K_p - G \\ b &= -[\gamma_1 K_w + G(\gamma_{HA}K_a + \gamma_{HB}K_b + \gamma_{HP}K_p) + r_1 + r_2 \\ &\quad + r_3 - \gamma_{HA}K_a(\gamma_{HB}K_b + \gamma_{HP}K_p) - \gamma_{HB}\gamma_{HP}K_bK_p] \\ c &= -\{r_1(\gamma_{HB}K_b + \gamma_{HP}K_p) + r_2(\gamma_{HA}K_a + \gamma_{HP}K_p) \\ &\quad + r_3(\gamma_{HA}K_a + \gamma_{HB}K_b) + \gamma_1 K_w(\gamma_{HA}K_a + \gamma_{HB}K_b \\ &\quad + \gamma_{HP}K_p) + G[\gamma_{HA}K_a(\gamma_{HB}K_b + \gamma_{HP}K_p) \\ &\quad + \gamma_{HB}\gamma_{HP}K_bK_p] - \gamma_{HA}\gamma_{HB}\gamma_{HP}K_aK_bK_p\} \\ d &= -\{\gamma_1 K_w[\gamma_{HA}K_a(\gamma_{HB}K_b + \gamma_{HP}K_b) + \gamma_{HB}\gamma_{HP}K_pK_b] \\ &\quad + G\gamma_{HA}\gamma_{HB}\gamma_{HP}K_aK_bK_p + r_1\gamma_{HB}\gamma_{HP}K_bK_p \\ &\quad + r_2\gamma_{HA}\gamma_{HP}K_aK_p + r_3\gamma_{HA}\gamma_{HB}K_aK_b\} \\ e &= -\gamma_1\gamma_{HA}\gamma_{HB}\gamma_{HP}K_wK_aK_bK_p \\ G &= [H^+]_b - \gamma_1[OH^-]_b - \gamma_2[A^-]_b - \gamma_3[B^-]_b - \gamma_4[P^-]_b \\ r_1 &= \gamma_3K_a[HA]_T = \gamma_3K_a(C_3 + C_4/r)/D_{HA} \\ r_2 &= \gamma_4[HB]_{T,b}K_b \\ r_3 &= \gamma_5K_p[HP]_T = \gamma_5K_p(C_1 + C_2/r)/D_{HP} \end{aligned} \tag{94}$$

Solution of the fifth-order equation can be done numerically by the Newton–Raphson method (26).

ACKNOWLEDGMENT

This project was partially supported by Colorcon, Inc.

NOMENCLATURE

a, b, c, d, e	= polynomial constants
$\mathbf{A}$	= stoichiometric coefficient matrix
C	= concentration
$\mathbf{C}$	= concentration matrix
$C_1, C_2, \ldots, C_8$	= integration constants
D	= diffusion coefficient in stagnant film
D'	= diffusion coefficient in the polymer matrix
h	= initial polymer thickness, $R_2 - R_1$
J	= dissolution flux
K_a	= equilibrium constant for drug
K_b	= equilibrium constant for buffer
K_p	= equilibrium constant for polymer
K_w	= equilibrium constant for water
k_s	= mass transfer coefficient
r	= radial coordinate
R_1, R	= radius for drug core and polymer, respectively
q	= diffusivity ratio
t	= time
$\mathbf{v}$	= velocity vector
x	= dimensionless coordinte, $(r - R_1)/(h + \delta)$
X	= chemical species, general
Y	= acid conjugate, general; see Eq. (38)

Greek

α	= parameter defined by Eq. (61)
δ	= film thickness
γ_1	= diffusivity ratio, D_{OH^-}/D_{H^+}
γ_2	= diffusivity ratio, D_{A^-}/D_{H^+}, for acids
$\gamma_{HA}, \gamma_{HB}, \gamma_{HP}$	= diffusivity ratio
ρ	= density
ρ_M	= molal density
ϕ	= reaction rate in the stagnant film
ϕ'	= reaction rate in the polymer matrix
∇	= gradient operator
∇^2	= Laplace operator
ν	= kinematic viscosity
ν	= stoichiometric coefficient
ω	= angular velocity

Subscripts

b	= bulk
o	= initial, intrinsic
s	= surface
T	= total
p	= polymer

REFERENCES

1. S. C. Porter and K. Ridgeway. *J. Pharm. Pharmacol.* **34**:5–8 (1982)
2. W. G. Chambliss. *Pharm. Tech.* **7**:124–140 (1983).
3. K. S. Murhty, N. A. Enders, M. Mahjour, and M. B. Fawzi. *Pharm. Tech.* **10**:36–46 (1986).
4. USP Convention. *United States Pharmacopeia,* 21st ed., USP Convention, Rockville, Md., 1985, Suppl. 3.
5. C. Y. Lui, D. D. Cilla, S. C. Porter, and J. B. Dressman. *APhA Acad. Pharm. Sci.* **15**:88–88 (1985).
6. W. Nernst. *Z. Phys. Chem.* **47**:52–55 (1904).
7. E. Brunner, *Z. Phys. Chem.* **47**:56–102 (1904)
8. W. I. Higuchi, L. Parrott, D. E. Wurster, and T. Higuchi. *J. Am. Pharm. Assoc.* **47**:376–383 (1958).
9. W. I. Higuchi, E. Nelson, and J. G. Wagner. *J. Pharm. Sci.* **53**:333–335 (1965).
10. K. G. Mooney, M. A. Mintun, K. J. Himmelstein, and V. J. Stella. *J. Pharm. Sci.* **70**:13–21 (1981).
11. K. G. Mooney, M. A. Mintun, K. J. Himmelstein, and V. J. Stella. *J. Pharm. Sci.* **70**:22–32 (1981).
12. S. S. Ozturk, B. O. Palsson, and J. B. Dressman. *Pharm. Res.* **5**:272–282 (1988).
13. J. Heller, R. W. Baker, R. M. Gale, and J. O. Rodin. *J. Appl. Polymer Sci.* **22**:1991–2009 (1978).

14. J. Spitael and R. Kinget. *Pharm. Ind.* 39:502–505 (1977).
15. J. Spitael, R. Kinget, and K. Naessens. *Pharm. Ind.* 42:846–849 (1980).
16. D. P. McNamara and G. L. Amidon. *J. Pharm. Sci.* 75:858–868 (1986).
17. J. B. Dressman and G. L. Amidon. *J. Pharm. Sci.* 73:935–936 (1984).
18. C. A. Youngberg, R. R. Berardi, W. F. Howatt, M. L. Hyneck, G. L. Amidon, J. H. Meyer, and J. B. Dressman. *Digest. Dis. Sci.* 32:472–480 (1986).
19. J. R. Malagelada, G. F. Longstreth, W. H. J. Summerskill, and V. L. W. Go. *Gastroenterology* 70:203 (1976).
20. P. M. Christiansen. *Scand. J. Gastroenterol.* 3:497–508 (1968).
21. J. D. Maxwell, A. Ferguson, and W. C. Watson. *Digestion* 4:345–352 (1971).
22. S. C. Porter. Personal communication, Colorcon, Inc.
23. M. Davis, I. Ichikawa, E. J. Williams, and G. S. Banker. *Int. J. Pharm.* 28:157–166 (1986).
24. T. K. Sherwood, R. L. Pigford, and C. R. Wilke. *Mass Transfer,* McGraw–Hill, New York, 1975.
25. C. G. Hill, Jr. *An Introduction to Chemical Engineering Kinetics and Reactor Design,* John Wiley and Sons, New York, 1977.
26. B. Carnahan, H. A. Luther, and J. O. Wilkes. *Applied Numerical Methods,* Wiley, New York, 1969.